

## Piezoelectric–piezomagnetic multilayer with simultaneously negative permeability and permittivity

H. Liu, S. N. Zhu,<sup>a)</sup> Y. Y. Zhu, Y. F. Chen, and N. B. Ming  
*Department of Physics, National Laboratory of Solid State Microstructures,  
 Nanjing University, Nanjing 210093, People's Republic of China*

X. Zhang  
*Mechanical and Aerospace Engineering, University of California, Los Angeles, Los Angeles,  
 California 90095*

(Received 16 July 2004; accepted 28 December 2004; published online 1 March 2005)

We study the propagation of an electromagnetic (EM) wave in piezoelectric–piezomagnetic multilayers, in which the incident EM wave excites high frequency acoustic waves and couples strongly with them through piezoelectric and piezomagnetic effects, creating dielectric polariton and magnetic polariton simultaneously. The dispersion abnormality appears at some frequency ranges where simultaneous negative permittivity and permeability can be achieved. Theoretical analysis and numerical simulation proved that this structure forms a kind of “left-handed” material. © 2005 American Institute of Physics. [DOI: 10.1063/1.1868073]

A medium having both  $\epsilon$  and  $\mu$  negative (called left-handed material) has dramatically different propagation characteristics stemming from the sign change of the group velocity, including reversal of both the Doppler shift and Cherenkov radiation, anomalous refraction, and even reversal of radiation pressure to radiation tension.<sup>1</sup> In recent work, a new kind of material (called metamaterial), combining a lattice of metallic wires<sup>2</sup> with a lattice of split ring resonators,<sup>3</sup> exhibits a frequency region in the microwave region with simultaneously negative values of effective permeability  $\mu_{\text{eff}}(\omega)$  and permittivity  $\epsilon_{\text{eff}}(\omega)$ , which can constitute left-handed material (LHM).<sup>4</sup> At present, the reality of left-handed material (LHM) has been verified by some experiments<sup>5,6</sup> and numerical simulation.<sup>7</sup> LHM is attracting growing interest in both theoretical and experimental research. Various interesting physical properties of LHM structures were discussed, such as negative refraction,<sup>8</sup> imaging of superlens,<sup>9</sup> enhancement of evanescent wave,<sup>10</sup> and so on. Furthermore, some nano-scale metamaterial has been successfully fabricated which can realize plasmonic resonance<sup>11</sup> and magnetic resonance<sup>12</sup> in terahertz frequency range.

Recently, a coupling between the superlattice vibrations and the electromagnetic (EM) wave was established in piezoelectric superlattice,<sup>13–15</sup> in which piezoelectric coefficient is modulated. This coupling produced a new type of polariton, in which negative effective permittivity  $\epsilon_{\text{eff}}(\omega)$  can be obtained near the high frequency side of the resonance. On the other hand, considerable research has been directed toward the development of piezoelectric–piezomagnetic composite materials that are defined as the combination of distinct phases of piezoelectric and piezomagnetic materials.<sup>16–18</sup> In piezoelectric–piezomagnetic multilayer composite (PPC), piezoelectric coefficient and piezomagnetic coefficient are modulated simultaneously. The lattice vibration will couple with the EM wave through piezoelectric effect and piezomagnetic effect, and dielectric polariton and magnetic polariton can be induced in PPC medium at the same time. Then can simultaneously negative  $\epsilon_{\text{eff}}(\omega)$  and  $\mu_{\text{eff}}(\omega)$  be produced

in this PPC medium? The problem is treated theoretically in this letter and a LHM medium can be constructed in such structure, as demonstrated in the following.

In order to elucidate the above-mentioned idea, let us consider an one-dimensional periodic structure composed of alternating layers of LiNbO<sub>3</sub> (piezoelectric) and CoFe<sub>2</sub>O<sub>4</sub> (piezomagnetic) arranged along the  $x$  axis. The thicknesses of the piezoelectric and piezomagnetic layers are the same ( $d$ ). Figure 1 is a schematic diagram of the case. Here only three periods of the PPC have been shown. Also we assume that the transverse dimensions are very large compared with an acoustic wavelength so that a one-dimensional model is applicable. When EM wave is radiated into this PPC multilayer along the  $x$  axis, with electric field in  $y$  direction and magnetic field in  $z$  direction, a longitudinal acoustic wave (LAW) propagating along the  $x$  axis will be excited through piezoelectric effect and piezomagnetic effect at the same time. The coupled interaction between the EM wave and acoustic wave can be described by constitutive equations:

$$T_1 = C_{11}^E S_1 + e_{22}(x)E_2 - q_{31}(x)H_3,$$

$$P_2 = \epsilon_0(\epsilon_{11}^s - 1)E_2 - e_{22}(x)S_1, \quad (1)$$

$$M_3 = \mu_0(\mu_{33}^s - 1)H_3 + q_{31}(x)S_1,$$

where  $T_1$ ,  $S_1$ ,  $C_{11}^E$ ,  $E_2$ ,  $P_2$ ,  $H_3$ , and  $M_3$  are the stress, strain, elastic coefficient, electric field, polarization, magnetic field, and magnetization, respectively.  $\epsilon_{11}^s$  and  $\mu_{33}^s$  are static permittivity and static permeability of multilayers which can be derived by applying the averaged field method.<sup>19,20</sup>  $e_{22}(x)$  and  $q_{31}(x)$  are piezoelectric coefficient and piezomagnetic coefficient. In piezoelectric layers LiNbO<sub>3</sub> ( $0 \leq x < d$ ),  $e_{22}(x) = e_{22} = 1.7 \text{ C/m}^2$  and  $q_{31}(x) = 0$ , while in piezomagnetic layers CoFe<sub>2</sub>O<sub>4</sub> ( $d \leq x < \Lambda = 2d$ ),  $e_{22}(x) = 0$  and  $q_{31}(x) = q_{31} = 850 \text{ N/A m}$ . By using the Fourier transformation,  $e_{22}(x)$  and  $q_{31}(x)$  can be expanded as

<sup>a)</sup>Electronic mail: zhusn@nju.edu.cn

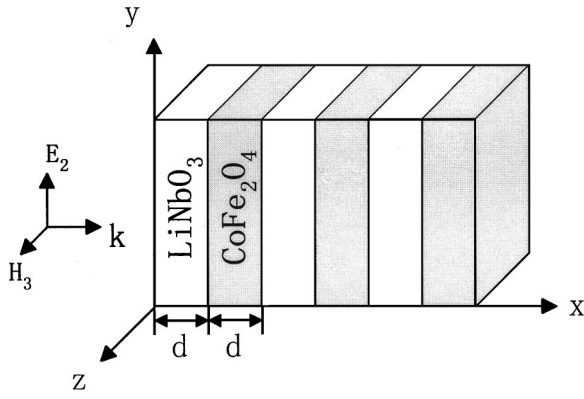


FIG. 1. Schematic illustration of the piezoelectric–piezomagnetic multilayers.

$$e_{22}(x) = \sum_{m \neq 0} \frac{i(1 - \cos m\pi)e_{22}}{2m\pi} e^{-iG_m x},$$

$$q_{31}(x) = \sum_{m \neq 0} \frac{i(1 - \cos m\pi)q_{31}}{2m\pi} e^{-iG_m x}$$

( $G_m = m\pi/d, m = 1, 3, 5, \dots$ ).

With the use of Newton’s law, the equation of motion for a vibrating medium can be obtained

$$\rho \frac{\partial^2 S_1}{\partial t^2} - C_{11}^E \frac{\partial^2 S_1}{\partial x^2} = \frac{\partial^2}{\partial x^2} (-e_{22}(x)E_2 + q_{31}(x)H_3),$$

where  $\rho$  is the mass density. Equation (3) indicates that the PPC is a forced oscillator. That is, a LAW propagating along the  $x$  axis will be excited by a transverse EM wave. The frequency of the acoustical wave will be that of the EM wave.

Here, we deal with the piezoelectric–piezomagnetic multilayer model with the same mathematical method used in Refs. 14 and 15. The long wavelength approximation (the wavelength of photon is much larger than the period of

multilayer) is still applicable in this model. The dispersion of effective permittivity and effective permeability can be attained as

$$\epsilon(\omega)\epsilon_{11}^s + \sum_m \frac{e_{22}^2/(d^2\rho\epsilon_0)}{\omega_m^2 - \omega^2},$$

$$\mu(\omega) = \mu_{33}^s + \sum_m \frac{q_{31}^2/(d^2\rho\mu_0)}{\omega_m^2 - \omega^2},$$

where  $\omega_m = G_m v_a (m = 1, 3, 5, \dots)$ , the resonance frequency due to the coupling between the EM wave and LAW;  $v_a = \sqrt{C_{11}^S/\rho}$  represents the velocity of the acoustic wave. From Eq. (4), we can see that  $\epsilon(\omega)$  and  $\mu(\omega)$  have the same resonance frequencies. Each resonance frequency  $\omega_m$  is related to one reciprocal vector  $G_m$ . If the frequency of the incident EM wave is near the frequency  $\omega_1$  that is related to the first-order reciprocal vector  $G_1 = \pi/d$ , the contribution of other high-order reciprocal vectors on the dispersion function can be ignored, then

$$\epsilon(\omega) = \epsilon_{11}^s + \frac{e_{22}^2/(d^2\rho\epsilon_0)}{\omega_1^2 - \omega^2}, \quad \mu(\omega) = \mu_{33}^s + \frac{q_{31}^2/(d^2\rho\mu_0)}{\omega_1^2 - \omega^2}.$$

The dispersion of wave vector due to the coupling between EM wave and LAW can be deduced from Eq. (5) and Maxwell’s equations,

$$\frac{c^2 k^2}{\omega^2} = \left( \epsilon_{11}^s + \frac{e_{22}^2/(d^2\rho\epsilon_0)}{\omega_1^2 - \omega^2} \right) \left( \mu_{33}^s + \frac{q_{31}^2/(d^2\rho\mu_0)}{\omega_1^2 - \omega^2} \right),$$

where  $c$  is the EM wave velocity in vacuum.

In the piezoelectric–piezomagnetic multilayer, the elastic coefficient  $C_{11}^E = 250$  GPa, static permittivity  $\epsilon_{11}^s/\epsilon_0 = 25$ , static permeability  $\mu_{33}^s/\mu_0 = 53$ , mass density  $\rho = 5.0 \times 10^3$  kg/m<sup>3</sup>. The thickness of each layer is  $d = 50$  nm and the first-order reciprocal vector of this periodic structure can be attained as  $G = \pi/d = 6.283 \times 10^7$  m<sup>-1</sup>, and the first resonance frequency  $\omega_1 = 4.44 \times 10^{11}$  Hz. The wavelength of EM wave at  $\omega_1$  is  $670 \mu\text{m} \gg d$ , then the long wavelength ap-

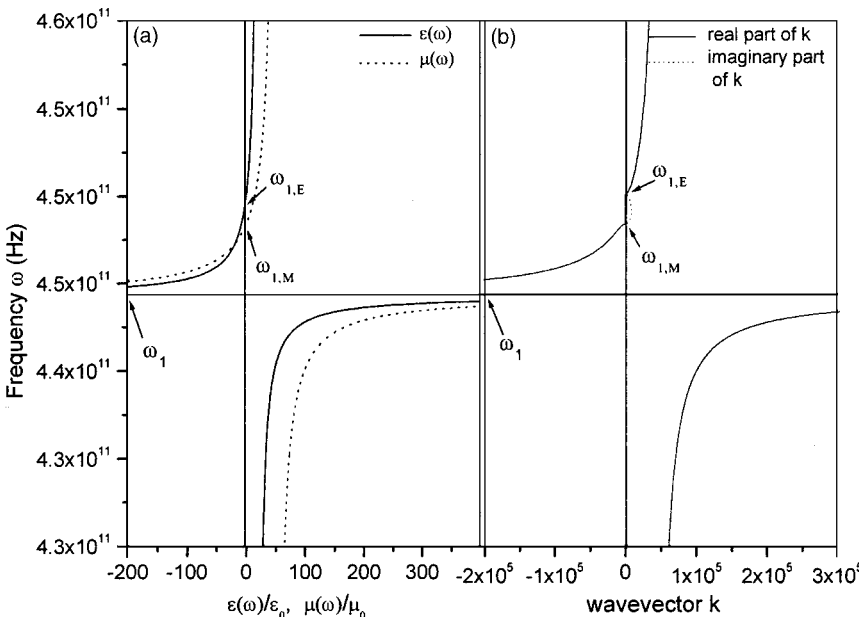


FIG. 2. The abnormal dispersion relationship of permittivity, permeability, and wave vector near resonance frequency.

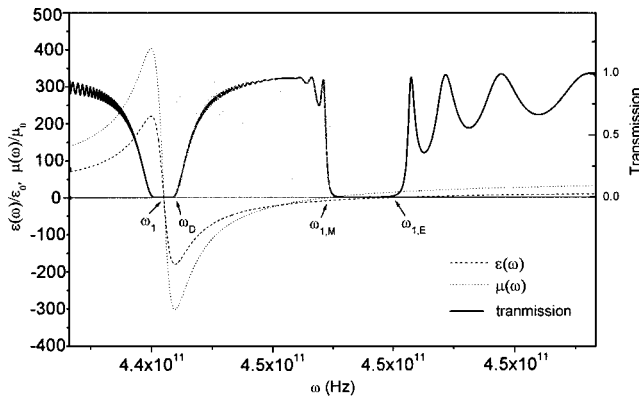


FIG. 3. Numerical calculated transmission curve of 200-period LiNbO<sub>3</sub>/CoFe<sub>2</sub>O<sub>4</sub> PPC multilayers.

proximation used in this model is valid. Figures 2(a) and 2(b) show the coupled modes of photons and lattice vibration in the PPC multilayers described by Eqs. (5) and (6). At the resonance frequency the photon–phonon coupling entirely changes the character of the propagation of EM wave. In the resonance region the propagation is neither a pure photon mode nor a pure longitudinal phonon mode. The quantum of the coupled photon–phonon wave field is called a polariton. For PPC multilayer, dielectric polariton and magnetic polariton are formed simultaneously near frequency  $\omega_1$ . One effect of the coupling is to create a frequency gap above the frequency  $\omega_1$ . By setting  $\varepsilon(\omega)=0$  and  $\mu(\omega)=0$  in Eq. (5), the upper cutoff frequency of dielectric polariton and magnetic polariton can be calculated as  $\omega_{1,E}=4.50 \times 10^{11}$  Hz and  $\omega_{1,M}=4.48 \times 10^{11}$  Hz. As shown in Fig. 2(b), for the frequencies  $\omega_{1,M} < \omega < \omega_{1,E}$ ,  $\varepsilon(\omega)$  has negative value while  $\mu(\omega)$  has positive value, the wave vector  $k$  is pure imaginary and the incident radiation with these frequencies will be reflected. For the overlapping region  $\omega_1 < \omega < \omega_{1,M}$ , both  $\varepsilon_{11}(\omega)$  and  $\mu_{33}(\omega)$  have negative values and the wave vector is also negative  $k < 0$ . As the group velocity is defined as the slope ratio of the dispersion curve  $d\omega/dk$  and the phase velocity is defined as the direct ratio  $\omega/k$ , it can be found that group velocity is maintained positive while the phase velocity changes to negative in  $\omega_1 < \omega < \omega_{1,M}$ , which can be seen obviously in Fig. 2(b). The effect of phase and group velocity propagating in opposite direction illustrates that PPC multilayer produces a resultant left-handed material.

Numerical simulations were carried out to calculate the transmittance of multilayer structure, in which 200-period PPC sample is taken as an example. Transfer matrix method is applied and the results of this simulation are shown in Fig. 3. Material loss is taken into consideration and viscoelastic damping magnitude is  $\eta=74.4 \times 10^{-5}$  Nm/s<sup>2</sup>, which is neglected by both Eqs. (5) and (6). In Fig. 3, with frequency approximating  $\omega_1$ , the coupling between the EM wave and acoustic wave will become stronger and the loss of transmission caused by damping will become greater. For the frequency  $\omega_1 < \omega < \omega_D=4.446 \times 10^{11}$  Hz, the damping is so great that the EM wave is completely absorbed. In the band

gap  $\omega_{1,M} < \omega < \omega_{1,E}$ , permittivity is negative and permeability is positive. The wave vector becomes imaginary and the incident radiation with these frequencies are reflected. Therefore, in the resonance region, only frequencies in  $\omega_D < \omega < \omega_{1,M}$  can pass through the sample overcoming absorption and reflection which is shown as the shadow region in Fig. 3. This passband indicates that the negative permittivity and permeability have combined to allow propagation.

In this letter, we only consider the normal incidence case of the EM wave in the PPC multilayer. If EM wave is radiated into the PPC multilayer with an oblique angle, EM wave will not only couple with the longitudinal acoustic wave along the  $x$  axis but also couple with the transverse acoustic wave in the  $y$ – $z$  plane. In following letters, we will extend the above-mentioned model to prove that simultaneous negative permittivity and permeability can also be obtained in the oblique incidence case. Some properties of the PPC structure, such as negative refraction, imaging of superlens, enhancement of evanescent wave, will also be studied.

The authors thank S. Y. Zhang and R. X. Wu for useful discussion. This work is supported by grants for the State Key Program for Basic Research of China, and by the National Natural Science Foundation of China under Contract No. 90201008 and of Jiangsu Planned Projects for Postdoctoral Research Funds.

<sup>1</sup>V. G. Veselago, Sov. Phys. Usp. **10**, 509 (1968).

<sup>2</sup>J. B. Pendry, A. J. Holden, W. J. Stewart, and I. Youngs, Phys. Rev. Lett. **76**, 4773 (2000)

<sup>3</sup>J. B. Pendry, A. J. Holden, D. J. Robbins, and W. J. Stewart, IEEE Trans. Microwave Theory Tech. **47**, 2075 (1999)

<sup>4</sup>D. R. Smith, W. J. Padilla, D. C. Vier, S. C. Nemat-Nasser, and S. Schultz, Phys. Rev. Lett. **84**, 4184 (2000).

<sup>5</sup>R. A. Shelby, D. R. Smith, and S. Schultz, Science **292**, 77 (2001).

<sup>6</sup>A. A. Houck, J. B. Brock, and I. L. Chuang, Phys. Rev. Lett. **90**, 137401 (2003).

<sup>7</sup>S. Foteinopoulou, E. N. Economou, and C. M. Soukoulis, Phys. Rev. Lett. **90**, 107402 (2003).

<sup>8</sup>D. R. Smith and D. Schurig, Phys. Rev. Lett. **90**, 077405 (2003).

<sup>9</sup>N. Fang and X. Zhang, Appl. Phys. Lett. **82**, 161 (2003).

<sup>10</sup>Z. W. Liu, N. Fang, T. J. Yen, and X. Zhang, Appl. Phys. Lett. **83**, 5184 (2003).

<sup>11</sup>D. M. Wu, N. Fang, C. Sun, X. Zhang, W. J. Padilla, D. N. Basov, D. R. Smith, and S. Schultz, Appl. Phys. Lett. **83**, 201 (2003).

<sup>12</sup>T. J. Yen, W. J. Padilla, N. Fang, D. C. Vier, D. R. Smith, J. B. Pendry, D. N. Basov, and X. Zhang, Science **303**, 1494 (2004).

<sup>13</sup>Y. Q. Lu, Y. Y. Zhu, Y. F. Chen, S. N. Zhu, N. B. Ming, and Y. J. Feng, Science **284**, 1822 (1999).

<sup>14</sup>Y. Y. Zhu, X. J. Zhang, Y. Q. Lu, Y. F. Chen, S. N. Zhu, and N. B. Ming, Phys. Rev. Lett. **90**, 053903 (2003).

<sup>15</sup>X. J. Zhang, R. Q. Zhu, J. Zhao, Y. F. Chen, and Y. Y. Zhu, Phys. Rev. B **69**, 085118 (2004).

<sup>16</sup>C. W. Nan, Phys. Rev. B **50**, 6082 (1994).

<sup>17</sup>M. I. Bichurin, I. A. Kornev, V. M. Petrov, A. S. Tatarenko, Yu. V. Kiliba, and G. Srinivasan, Phys. Rev. B **64**, 094409 (2001).

<sup>18</sup>M. I. Bichurin, V. M. Petrov, Yu. V. Kiliba, and G. Srinivasan, Phys. Rev. B **66**, 134404 (2002).

<sup>19</sup>V. M. Agranovich and V. E. Kravtsov, Solid State Commun. **55**, 85 (1985).

<sup>20</sup>F. G. Elmzoughi, N. C. Constantinou, and D. R. Tilley, Phys. Rev. B **51**, 11515 (1995).